nature chemistry

ARTICLES

PUBLISHED ONLINE: 29 MAY 2017 | DOI: 10.1038/NCHEM.2783

Enantioselective, intermolecular benzylic C–H amination catalysed by an engineered iron-haem enzyme

Christopher K. Prier†, Ruijie K. Zhang†, Andrew R. Buller, Sabine Brinkmann-Chen and Frances H. Arnold*

C–H bonds are ubiquitous structural units of organic molecules. Although these bonds are generally considered to be chemically inert, the recent emergence of methods for C–H functionalization promises to transform the way synthetic chemistry is performed. The intermolecular amination of C–H bonds represents a particularly desirable and challenging transformation for which no efficient, highly selective, and renewable catalysts exist. Here we report the directed evolution of an iron-containing enzymatic catalyst—based on a cytochrome P450 monooxygenase—for the highly enantioselective intermolecular amination of benzylic C–H bonds. The biocatalyst is capable of up to 1,300 turnovers, exhibits excellent enantioselectivities, and provides access to valuable benzylic amines. Iron complexes are generally poor catalysts for C–H amination: in this catalyst, the enzyme's protein framework confers activity on an otherwise unreactive iron-haem cofactor.

C–H bonds may be the most common functional groups in organic molecules but are typically considered inert toward chemical transformation. By selectively acting on these bonds and installing new functional groups directly into the hydrocarbon framework of organic compounds, C–H functionalization technology has the potential to streamline synthetic routes, leading to less wasteful and more sustainable chemical production[1–3]. Modern C–H functionalization methods, however, rely heavily on catalytic complexes of precious transition metals (such as rhodium, ruthenium and iridium), which are neither cheap nor green[1]. Many enzymes, by contrast, catalyse very challenging reactions using base metals; their activities are often only possible because the protein plays a key role, modifying or enhancing the inherent reactivity of the metal cofactor[4]. We envisioned that enzymes dependent only on base metals could be exploited through reaction design and evolution to perform non-biological C–H functionalization reactions, potentially with efficiencies and selectivities exceeding those of known chemical catalysts.

Due to the presence of nitrogen in many bioactive synthetic and natural compounds, methods for directly transforming sp^3-hybridized C–H bonds into C–N bonds have been pursued intensively[5–9]. Many of the methods that have been developed are either intramolecular (requiring that a nitrogen source already be present in the same molecule as the targeted C–H bond) or utilize directing groups (also requiring the presence of specific functionality in the starting material). An elegant yet more elusive transformation is the intermolecular C–H amination of unfunctionalized hydrocarbons; such a reaction provides a dramatically simplifying and convergent disconnection for the synthesis of amines from alkanes (Fig. 1). Recognizing the potential of this transformation, several groups have pursued innovative strategies for intermolecular C–H amination. While many of these methods are racemic[10–14], enantioselective intermolecular C–H amination via the generation and transfer of metal nitrenoids has been developed using rhodium[15–17], ruthenium[18,19] and manganese[19,20] catalysts. Highly diastereoselective C–H amination using a chiral nitrogen source has also been achieved using a rhodium catalyst[21]. These systems represent major advances in C–H functionalization; none, however, offer the combination of high catalytic efficiency (turnover), high enantioselectivity across diverse substrates, and ready access to the chiral catalyst.

Cytochrome P450 monooxygenases are nature's catalysts for the direct insertion of oxygen into C–H bonds. These iron-dependent enzymes perform hydroxylation with high reaction rates and turnovers, and do so under mild physiological conditions[22]. They also act with excellent selectivity in complex settings, often hydroxylating only one C–H bond out of many in diverse secondary metabolites[23]. In contrast to this strategy for oxygenation, nature does not introduce nitrogen into organic molecules via C–H functionalization. Biosynthetic routes to amines instead rely exclusively on functional group manipulation of pre-oxidized substrates, and biocatalytic multi-enzyme cascades have been engineered for formal C–H amination using this general approach[24,25].

In striking contrast to both natural and synthetic amination strategies, it has been shown that haem proteins can catalyse nitrene transfer under appropriate reaction conditions[26–32]. In particular, variants of cytochrome $P450_{BM3}$ from *Bacillus megaterium* that feature a serine axial ligand to the haem iron in place of the wild-type cysteine ligand, which we term cytochrome P411s (ref. 33), are proficient catalysts for nitrene transfer. Based on this manifold, we envisioned the catalytic cycle for intermolecular amination shown in Fig. 2. First, reduction of the ferric state of the haem cofactor, with electrons derived from NADPH, gives the ferrous state **1**. Reaction with a nitrene source, here tosyl azide (TsN_3), then provides the putative iron nitrenoid **2**. Subsequent reaction of this intermediate with an alkane such as 4-ethylanisole (**3**) would deliver the C–H amination product **4** and regenerate the ferrous state of the catalyst (**1**). A competing process observed in P411-catalysed

Division of Chemistry and Chemical Engineering, California Institute of Technology, 1200 East California Boulevard, MC 210-41, Pasadena, California 91125, USA. †These authors contributed equally to this work. *e-mail: frances@cheme.caltech.edu

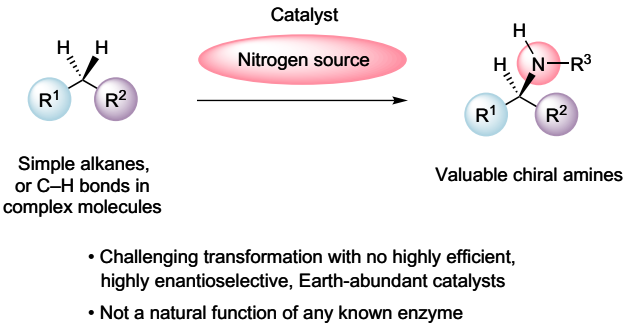

Figure 1 | Intermolecular C–H amination, a simplifying transformation for chiral amine synthesis. Intermolecular C–H amination enables direct and convergent functionalization in which a simple alkane and a nitrogen atom source are brought together in a single step. In principle, any C–H bond in the substrate is a potential site of functionalization.

nitrene transfer is the reduction of the nitrenoid, generating the undesired by-product *p*-toluenesulfonamide ($TsNH_2$, **5**). Cytochrome P411 catalysts have been identified for intramolecular C–H amination reactions[26,27]; in these cases, the targeted C–H bond is necessarily present in the enzyme active site when the reactive nitrenoid **2** is formed, biasing productive C–H amination over the deleterious nitrenoid reduction pathway. In contrast, a catalyst for the desired intermolecular amination must bind a separate alkane substrate and promote its amination faster than the transient nitrenoid species is consumed in the reductive side reaction.

Results and discussion

Reaction discovery and directed evolution. In initial studies, we found that almost all cytochrome P411s reported to date display no activity toward intermolecular C–H amination of alkane **3**—including catalysts that were developed for ostensibly similar reactions such as intramolecular C–H amination[26,27] and intermolecular aziridination[28]—instead they exclusively reduce the azide to the sulfonamide **5** (Supplementary Table 1). Other haem-containing proteins, as well as the haem cofactor alone (iron protoporphyrin IX), are similarly inactive (Supplementary Table 2). Remarkably, however, we found that $P411_{BM3}$ variant P-4, engineered for the imidation of allylic sulfides[29], shows promiscuous activity toward intermolecular C–H amination. Under anaerobic conditions, 4-ethylanisole (**3**) undergoes amination at the benzylic carbon in 11% yield and 14% e.e. by variant P-4, which differs from wild-type $P450_{BM3}$ by 17 mutations (Fig. 3). Even more encouragingly, a single mutation to P-4, A82L (also identified in the context of the sulfimidation reaction), provides a greater than fourfold improvement in yield (to 51%) and delivers the product **4** in 77% e.e. Similarities between the nitrene transfer transition states of the sulfimidation and C–H insertion reactions may account for why evolution for one reaction engendered activity toward the other, leading to variants with expanded promiscuous capabilities toward nitrene transfer.

We next performed sequential rounds of site-saturation mutagenesis of selected residues in P-4 A82L and screening to improve C–H amination activity and enantioselectivity. We targeted sites in the haem domain that were either previously shown to impact the activity and/or selectivity of P450s, residues that are highly conserved in P450s, or residues that were already mutated in P-4 relative to wild-type $P450_{BM3}$ (see Supplementary Information for details)[34]. The libraries were screened for enhanced C–H amination activity, and potential hits were subsequently evaluated for activity across a set of three substrates with different electronic demands for C–H amination: 4-ethylanisole (**3**), 4-ethyltoluene (**6**), and ethylbenzene (**7**, Fig. 3). Two mutations, A78V and F263L, improve activity and selectivity on all three substrates, yielding a catalyst that delivers the benzylic amine products as single enantiomers (>99% e.e.). A final mutation, E267D, is neutral with respect to the amination of 4-ethylanisole but provides a twofold improvement in the amination of ethylbenzene (**7**, to 15% yield), as well as improving the reaction yield and/or selectivity in the C–H amination of other substrates (Supplementary Table 6). We call this final variant $P411_{CHA}$, for 'cytochrome P411 C–H aminase'. Under the conditions employed for evolution, this catalyst generates the benzylic amine **4** in 66% yield, with >99% e.e. and 1,000 turnovers in whole *Escherichia coli* cells. While 4-ethylanisole is electronically activated toward C–H insertion[15], alkanes **6** and **7** are less activated and display much lower reactivity with the initial P411 variants. Over the course of evolution from variant P-4 to $P411_{CHA}$, the amination of 4-ethylanisole was improved by sixfold, while the effect on the amination of ethylbenzene was significantly greater (30-fold improvement). Thus, using an electronically activated substrate (4-ethylanisole) allowed the initial discovery of P411 C–H amination activity, from which variants that aminate inherently less-reactive alkanes were derived.

Subsequent studies revealed that $P411_{CHA}$ can support up to 1,300 turnovers (Table 1, entry 3), far exceeding the highest turnover number (TON) reported with any chiral transition metal complex for intermolecular, enantioselective C–H amination (the best reported is 85 TON using a chiral manganese porphyrin)[19]. The reaction was optimized for yield by employing two equivalents of tosyl azide; under these conditions, the product **4** is obtained in 86% yield, with >99% e.e. and 670 turnovers (Table 1, entry 8). In contrast to the reported chemical protocols, the reaction with $P411_{CHA}$ takes place in water at room temperature; the reaction can also proceed under aerobic conditions, but the yield is sevenfold higher using the optimal anaerobic conditions (Supplementary Table 7).

Substrate scope studies. Scope studies, carried out using the yield-optimized conditions, revealed that cytochrome $P411_{CHA}$ aminates a diverse set of arene-containing hydrocarbons. Substitution of the aromatic ring is tolerated at *para*, *meta* and *ortho* positions (Table 2,

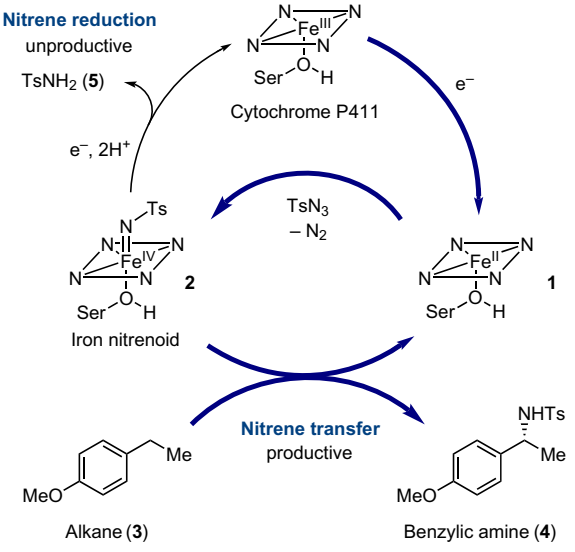

Figure 2 | Proposed mechanism of cytochrome P411-catalysed intermolecular C–H amination. Reaction of the aminating reagent, tosyl azide, with the ferrous porphyrin (**1**) generates an enzyme-bound iron nitrenoid intermediate (**2**). This nitrenoid then inserts into a C–H bond in the alkane, delivering a benzylic amine product. The nitrogen atoms in a plane represent the enzyme's haem cofactor. Ts, 4-toluenesulfonyl; Ser, serine.

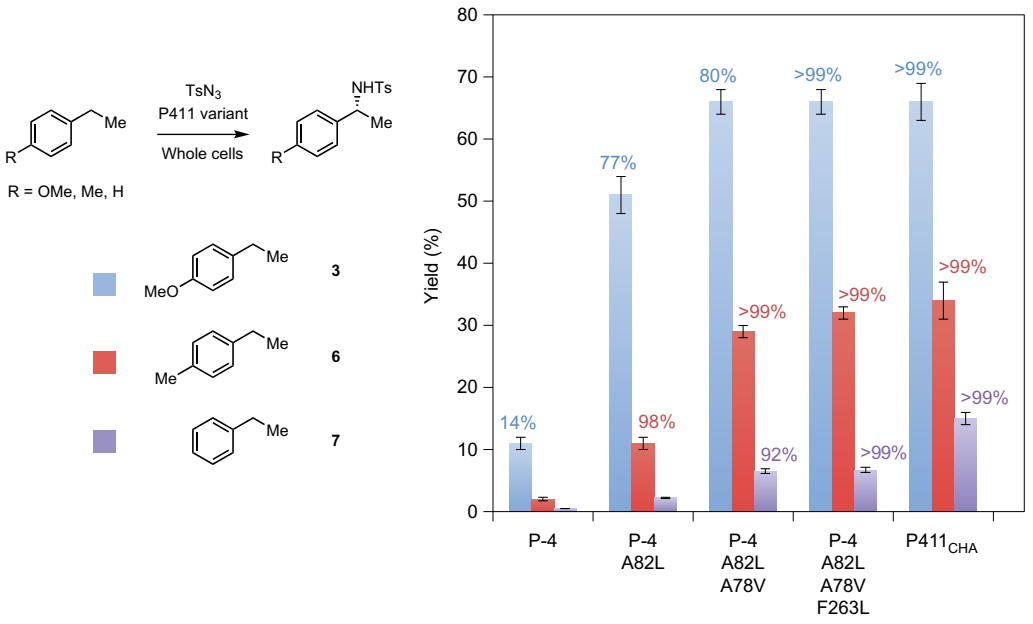

Figure 3 | Evolution of a cytochrome P411 catalyst for enantioselective C–H amination on increasingly challenging substrates. Directed evolution, via sequential rounds of site-saturation mutagenesis and screening, improved both the conversion and enantioselectivity of P411-catalysed C–H amination. The initial variant P-4 shows significant activity only on the electronically activated 4-ethylanisole (**3**); evolved variants display activity on inherently less-activated substrates. Reactions were performed using whole *E. coli* cells overexpressing the P411 variant, resuspended to OD_{600} = 30, with 5 mM alkane and 5 mM tosyl azide, under anaerobic conditions. Results are the average of experiments performed with duplicate cell cultures, each used to perform duplicate chemical reactions (four reactions total). Bars represent yield, and numbers above bars represent enantiomeric excess (e.e.); both are colour-coded to match the substrate (blue, 4-ethylanisole; red, 4-ethyltoluene; purple, ethylbenzene). Error bars correspond to one standard deviation. P-4 gives predominantly the *S* enantiomer in the amination of 4-ethylanisole (**3**); all other variant/substrate combinations give predominantly the *R* enantiomer.

entries 2–4). While electron-withdrawing functionality reduces the reactivity of the alkane toward the metal nitrenoid, several halogenated ethylbenzenes are nevertheless functionalized with >100 turnovers (entries 6–8). The cyclic alkanes indan and tetralin are excellent substrates (entries 9 and 10), while the related 2,3-dihydrobenzofuran displays reduced reactivity (entry 11). Larger alkylarenes such as ethylnaphthalenes and 4-propylanisole are still accommodated in the enzyme active site, undergoing amination with varying levels of efficiency (entries 12–14). Notably, the amination of 1-ethylnaphthalene delivers the nitrogen-containing fragment of the calcimimetic drug cinacalcet (Sensipar) with the correct absolute configuration (entry 13)[35]. Furthermore, although the activity is low, the amination of the methyl group of 4-methylanisole demonstrates that these catalysts are capable of functionalizing C–H bonds with bond dissociation energies as high as 90 kcal mol^{-1} (entry 15). Benzylic ethers are suitable substrates for amination, but the products are isolated in racemic form (entries 16–17). For the amination of isochroman (entry 17), analysis of crude reaction mixtures demonstrated that the C–H insertion event is moderately enantioselective (65% e.e.), but the product undergoes racemization during purification on silica gel (Supplementary Table 10).

Table 1 | Optimization of the $P11_{CHA}$-catalysed amination of 4-ethylanisole.

Entry	4-Ethylanisole (3; mM)	Tosyl azide (mM)	Yield (4)	TON
1*	5.0	5.0	66%	1,000
2	7.5	7.5	51%	1,200
3†	10	10	41%	1,300
4	15	15	26%	1,200
5	20	20	20%	1,200
6	2.5	2.5	56%	430
7	2.5	3.75	80%	630
8‡	2.5	5.0	86%	670
9	2.5	7.5	83%	640
10	2.5	10	78%	610

Reactions were performed with whole *E. coli* cells overexpressing $P411_{CHA}$, as in Fig. 3. All reactions generate benzylic amine **4** in >99% e.e. *Conditions employed during evolution. †Turnover-optimized conditions. ‡Yield-optimized conditions, employed for evaluating the substrate scope.

Notably, most of the alkanes evaluated undergo functionalization with excellent levels of enantioselectivity (>90% e.e.), a key advantage of this enzymatic approach over most reported metal catalysts. However, $P411_{CHA}$ displays several limitations with regard to substrate scope: it does not aminate substrates much larger than those shown here, nor does it functionalize benzylic positions adjacent to especially electron-deficient arenes (Supplementary Fig. 1). Interestingly, cumene and 4-methoxycumene are not aminated by $P411_{CHA}$ despite the presence of weak benzylic C–H bonds. We have also not found $P411_{CHA}$ to be active toward the amination of allylic or aliphatic C–H bonds, nor is it capable of aminating non-benzylic ethers. The aromatic motif may be required for productive substrate binding or to sufficiently lower the activation barrier of C–H insertion. Directed evolution, however, may improve the activities described here and alter the substrate scope of these enzymes, potentially by modifying the binding site of the alkane. Just as evolution within the functional space of nitrene transfer engendered expanded amination activities, it is possible that non-benzylic amination will be accessible to future generations of P411 enzymes. Cytochrome $P411_{CHA}$ also has improved thermostability relative to P-4 (T_{50} is increased by ~3 °C, to 61 °C, Supplementary Table 11), suggesting it may serve as a robust starting point for the evolution of specialized enantioselective C–H amination catalysts[36].

The enzymatic amination reaction can be performed on preparative scale: from a 0.25 mmol-scale biotransformation, the benzylic amine **4** was isolated in 78% yield (59.5 mg, 610 TON, >99% e.e.). The reaction also proceeds with purified protein, albeit less

Table 2 | Substrate scope of enzymatic intermolecular C–H amination.

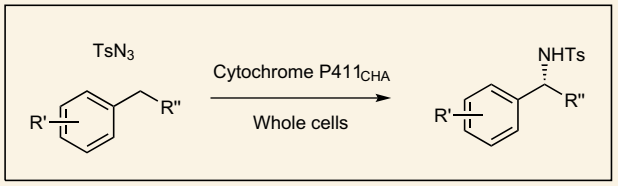

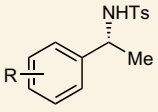

Entry **1:** R = *p*-OMe	86% yield, 670 TON, >99% e.e.
Entry **2:** R = *p*-Me	53% yield, 420 TON, >99% e.e.
Entry **3:** R = *m*-Me	58% yield, 460 TON, >99% e.e.
Entry **4:** R = *o*-Me	14% yield, 110 TON, 87% e.e.
Entry **5:** R = H	15% yield, 120 TON, >99% e.e.
Entry **6:** R = *p*-Br	19% yield, 150 TON, >99% e.e.
Entry **7:** R = *p*-Cl	19% yield, 150 TON, >99% e.e.
Entry **8:** R = *p*-F	22% yield, 170 TON, >99% e.e.

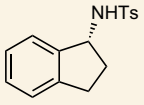

Entry **9:** 80% yield
640 TON, 96% e.e.

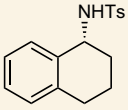

Entry **10:** 76% yield
660 TON, 95% e.e.

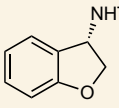

Entry **11:** 21% yield†
180 TON, 92% e.e.

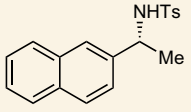

Entry **12:** 81% yield
710 TON, >99% e.e.

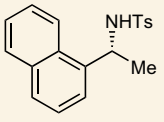

Entry **13:** 6% yield
45 TON, >99% e.e.

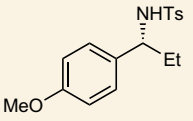

Entry **14:** 16% yield
140 TON, >99% e.e.

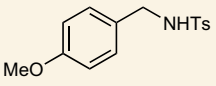

Entry **15:** 5% yield
47 TON

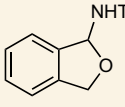

Entry **16:** 70% yield†
610 TON

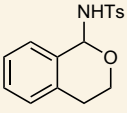

Entry **17:** 80% yield†
730 TON

Reactions were performed in duplicate with whole *E. coli* cells overexpressing $P411_{CHA}$ at OD_{600} = 30 (~3 μM enzyme), with 2.5 mM alkane and 5 mM tosyl azide. †Isolated yield from a reaction performed on 0.25-mmol scale (see Supplementary Information for details).

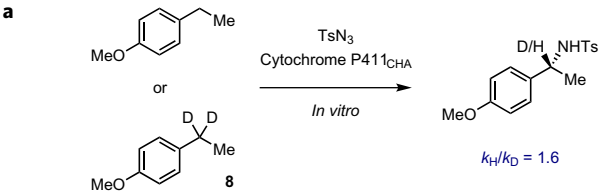

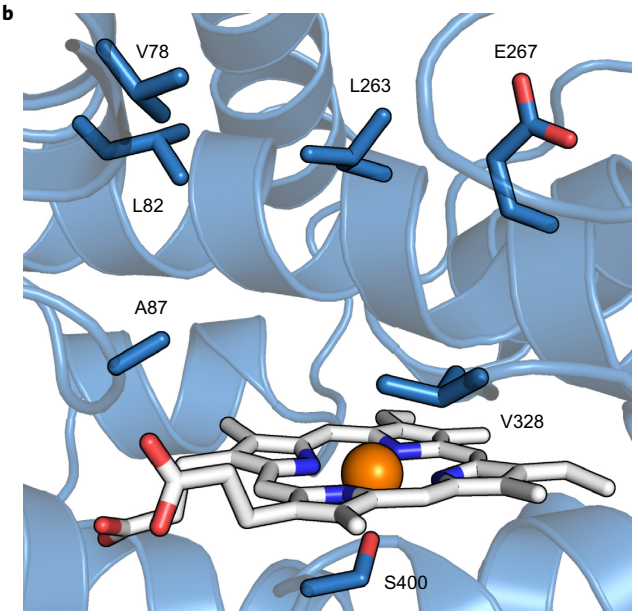

Figure 4 | Kinetic isotope effect and enzyme structural studies. a, The kinetic isotope effect in enzymatic C–H amination was determined from independent *in vitro* rate experiments. **b**, Active site view of the P-4 A82L A78V F263L crystal structure, showing the haem in white and the iron atom in orange. Key active site residues are labelled and shown as sticks in blue. Residue S400 ligates the iron centre; mutations at positions 78, 82, 263, and 267 enhance C–H amination activity and/or selectivity. All beneficial mutations identified in this study lie in the P411 active site on the distal face of the haem.

efficiently than in whole cells: the P411 catalysts are capable of up to 190 TON *in vitro* versus 1,300 TON *in vivo* (Supplementary Table 8). Furthermore, the tosyl group present in the C–H amination products may be removed via treatment with samarium diiodide[37], providing the corresponding primary amine with no erosion of enantiomeric excess (see Supplementary Information for details).

Rate experiments. The fact that amination activity throughout evolution is highly dependent on the electronic nature of the substrate (electron-rich substrates giving higher yields) suggests that C–H insertion is rate-determining. We questioned, however, whether improvements in yield arose from improved catalytic efficiency toward C–H amination or suppression of the competing azide reduction pathway (Fig. 2). Under *in vitro* conditions, initial rates are enhanced by greater than eightfold for the amination of 4-ethylanisole by $P411_{CHA}$ compared to P-4, showing that the mutations indeed increase the rate of the productive reaction (Supplementary Fig. 2). Independent rate measurements conducted with deuterated alkane **8** show a kinetic isotope effect (k_H/k_D) of 1.6 in the reaction catalysed by $P411_{CHA}$, suggesting only partial C–H bond cleavage in the amination transition state (Fig. 4a)[5], while also providing further evidence for a rate-determining C–H insertion event.

Crystallography. We obtained an X-ray crystal structure of the penultimate variant in our lineage (P-4 A82L A78V F263L) at 1.70-Å resolution (Fig. 4b). The beneficial mutations identified in this study are all located in helices that line the active site; two mutations are located in the enzyme's B′ helix (A82L, A78V) and two are located in the I helix (F263L, E267D). Residues in both of these helices are known to mediate substrate binding and/or impact selectivity in P450-catalysed oxygenation reactions[38–40]. Like two earlier reported P411 structures[27,33], the structure of the evolved aminase adopts the P450 closed state typically induced by substrate binding. Compared to the structure of P411 variant P-I263F (ref. 27), which differs by only six mutations yet performs intermolecular C–H amination with trace activity (<1% yield), there are only minor movements of the protein scaffold, although the active-site residue L437 surprisingly adopts an unfavoured backbone conformation. On average, the volume of the haem distal pocket is reduced by approximately 10% in the evolved variant compared to P-I263F; the smaller active site potentially enforces productive substrate binding modes. These

observations suggest that the mutations introduced on the path to $P411_{CHA}$ exert local effects that modulate interactions with the azide and alkane substrates in the active site. Docking simulations revealed plausible substrate conformations for nitrene transfer, in which the substrates are organized via van der Waals interactions with residues A87, L263, E267 and V328, among others (see Supplementary Information).

Conclusion

Cytochrome $P411_{CHA}$ displays the ability to aminate benzylic C–H bonds intermolecularly in diverse structures with high selectivity, demonstrating that a renewable protein catalyst based on iron (the most abundant transition metal in the Earth's crust) can solve a long-standing challenge in synthetic chemistry. The protein does more than simply control the reactivity of a reactive metal complex—as in the native P450 monooxygenation reaction, the protein enables a function that the iron cofactor cannot perform on its own. Biocatalysts for non-natural reactions have alternatively been created by introducing precious metals (such as iridium and rhodium) into proteins[41–43]. An artificial iridium metalloenzyme has been shown to perform nitrene transfer; this system is capable of up to ~300 turnovers in intramolecular C–H amination reactions[44]. That $P411_{CHA}$ achieves intermolecular C–H amination with the native iron cofactor suggests that costly precious metals—and strategies for introduction of the non-native metal—are not necessary to achieve highly active biocatalysts for challenging non-natural reactions. The current work also describes an evolutionary pathway in which P411s evolved for a more readily accessible nitrene transfer reaction (sulfimidation) picked up promiscuous activity toward a more challenging reaction (intermolecular C–H amination). This strategy of stepwise evolution through increasingly challenging reactivities may be generally useful for engineering enzymes for new activities not readily found by testing wild-type proteins. Finally, the ability to accelerate C–H insertion via mutation suggests that cytochrome $P411_{CHA}$ may be a platform for evolving catalysts for diverse C–H functionalization reactions currently inaccessible to chemical catalysis.

Methods

Expression of $P411_{BM3}$ variants. *E. coli* BL21 E. cloni cells carrying a plasmid encoding a P411 variant were grown overnight in 5 ml Luria-Bertani medium with 0.1 mg ml^{-1} ampicillin (LB_{amp}, 37 °C, 250 rpm). The preculture was used to inoculate 45 ml of Hyperbroth (HB) medium (prepared from AthenaES powder, 0.1 mg ml^{-1}ampicillin) in a 125 ml Erlenmeyer flask; this culture was incubated at 37 °C, 230 rpm for 2 h. Cultures were then cooled on ice (20 min), and expression was induced with 0.5 mM IPTG and 1.0 mM 5-aminolevulinic acid (final concentrations). Expression was conducted at room temperature (23 °C), at 130 rpm, for 16–18 h. Cultures were then centrifuged (2,600*g*, 10 min, 4 °C), and the pellets were resuspended to an OD_{600} of 30 in M9-N minimal media (no nitrogen). Aliquots of the cell suspension (4 ml) were used to determine the P411 expression level by CO-binding assay after lysis by sonication.

Intermolecular C–H amination in whole *E. coli* cells. For amination bioconversions, the cells containing the P411 variant, at OD_{600} of 30 in M9-N media (grown as described above), were degassed by sparging with argon in sealed 6-ml crimp vials for at least 40 min. Separately, a glucose solution (250 mM in M9-N) was degassed by sparging with argon for at least 10 min. An oxygen depletion system (20 µl of a stock solution containing 14,000 U ml^{-1} catalase and 1,000 U ml^{-1} glucose oxidase in 0.1 M KPi, pH 8.0) was added to 2-ml crimp vials. All solutions were uncapped and transferred into an anaerobic chamber. Resuspended cells (320 µl) were added to the vials, followed by glucose (40 µl, 250 mM in M9-N), alkane (10 µl of a DMSO stock), and tosyl azide (10 µl of a DMSO stock). Final concentrations were typically 2.5–5.0 mM alkane, 5.0 mM tosyl azide, and 25 mM glucose; final reaction volume was 400 µl. The vials were sealed, removed from the anaerobic chamber, and shaken at room temperature and 40 rpm for 16–20 h. The reactions were quenched by addition of acetonitrile (400 µl) and internal standard (10 µl of a DMSO stock). This mixture was then transferred to a microcentrifuge tube and centrifuged at 20,000*g* for 10 min. The supernatant was transferred to a vial and analysed by HPLC for yield. Reaction samples were extracted with cyclohexane and analysed by chiral SFC (supercritical fluid chromatography) for enantiomeric excess (e.e.). Yield is calculated as mM reaction product divided by mM alkane starting material; TON is calculated as mM reaction product divided by mM P411, as determined by the CO-binding assay following cell lysis. e.e. is calculated as (major enantiomer–minor enantiomer)/(major enantiomer + minor enantiomer).

Data availability. Complete experimental procedures, including synthesis methods for all compounds, characterization data, and details of bioconversion experiments are described in the Supplementary Information. The crystal structure of $P411_{BM3}$ P-4 A82L A78V F263L has been deposited in the Protein Data Bank (PDB) under accession code 5UCW.

Received 14 March 2017; accepted 21 April 2017; published online 29 May 2017

References

1. Hartwig, J. F. Evolution of C–H bond functionalization from methane to methodology. *J. Am. Chem. Soc.* **138,** 2–24 (2016).
2. Godula, K. & Sames, D. C–H bond functionalization in complex organic synthesis. *Science* **312,** 67–72 (2006).
3. Yamaguchi, J., Yamaguchi, A. D. & Itami, K. C–H bond functionalization: emerging synthetic tools for natural products and pharmaceuticals. *Angew. Chem. Int. Ed.* **51,** 8960–9009 (2012).
4. Bertini, I., Gray, H. B., Lippard, S. J. & Valentine, J. S. (eds) *Bioinorganic Chemistry* (University Science Books, 1994).
5. Zalatan, D. N. & Du Bois, J. Metal-catalyzed oxidations of C–H to C–N bonds. *Top. Curr. Chem.* **292,** 347–378 (2010).
6. Davies, H. M. L. & Manning, J. R. Catalytic C–H functionalization by metal carbenoid and nitrenoid insertion. *Nature* **451,** 417–424 (2008).
7. Collet, F., Lescot, C. & Dauban, P. Catalytic C–H amination: the stereoselectivity issue. *Chem. Soc. Rev.* **40,** 1926–1936 (2011).
8. Wu, W.-T., Yang, Z.-P. & You, S.-L. in *Asymmetric Functionalization of C–H Bonds* (ed. You, S.-L.) 1–66 (RSC Catalysis Series No. 25, 2015).
9. Jeffrey, J. L. & Sarpong, R. Intramolecular C(sp^3)–H amination. *Chem. Sci.* **4,** 4092–4106 (2013).
10. Ochiai, M., Miyamoto, K., Kaneaki, T., Hayashi, S. & Nakanishi, W. Highly regioselective amination of unactivated alkanes by hypervalent sulfonylimino-λ^3-bromane. *Science* **332,** 448–451 (2011).
11. Hennessy, E. T., Liu, R. Y., Iovan, D. A., Duncan, R. A. & Betley, T. A. Iron-mediated intermolecular N-group transfer chemistry with olefinic substrates. *Chem. Sci.* **5,** 1526–1532 (2014).
12. Sharma, A. & Hartwig, J. F. Metal-catalysed azidation of tertiary C–H bonds suitable for late-stage functionalization. *Nature* **517,** 600–604 (2015).
13. Huang, X., Bergsten, T. M. & Groves, J. T. Manganese-catalyzed late-stage aliphatic C–H azidation. *J. Am. Chem. Soc.* **137,** 5300–5303 (2015).
14. Michaudel, Q., Thevenet, D. & Baran, P. S. Intermolecular Ritter-type C–H amination of unactivated sp^3 carbons. *J. Am. Chem. Soc.* **134,** 2547–2550 (2012).
15. Nägeli, I. *et al.* Rhodium(II)-catalyzed CH Insertions with {[(4-Nitrophenyl) sulfonyl]imino}phenyl-λ^3-iodane. *Helv. Chim. Acta* **80,** 1087–1105 (1997).
16. Yamawaki, M., Tsutsui, H., Kitagaki, S., Anada, M. & Hashimoto, S. Dirhodium (II) tetrakis[*N*-tetrachlorophthaloyl-(*S*)-*tert*-leucinate]: a new chiral Rh(II) catalyst for enantioselective amidation of C–H bonds. *Tetrahedron Lett.* **43,** 9561–9564 (2002).
17. Reddy, R. P. & Davies, H. M. L. Dirhodium tetracarboxylates derived from adamantylglycine as chiral catalysts for enantioselective C–H aminations. *Org. Lett.* **8,** 5013–5016 (2006).
18. Nishioka, Y., Uchida, T. & Katsuki, T. Enantio- and regioselective intermolecular benzylic and allylic C–H bond amination. *Angew. Chem. Int. Ed.* **52,** 1739–1742 (2013).
19. Zhou, X.-G., Yu, X.-Q., Huang, J.-S. & Che, C.-M. Asymmetric amidation of saturated C–H bonds catalysed by chiral ruthenium and manganese porphyrins. *Chem. Commun.* 2377–2378 (1999).
20. Kohmura, Y. & Katsuki, T. Mn(salen)-catalyzed enantioselective C–H amination. *Tetrahedron Lett.* **42,** 3339–3342 (2001).
21. Liang, C. *et al.* Efficient diastereoselective intermolecular rhodium-catalyzed C–H amination. *Angew. Chem. Int. Ed.* **45,** 4641–4644 (2006).
22. Urlacher, V. B. & Girhard, M. Cytochrome P450 monooxygenases: an update on perspectives for synthetic application. *Trends Biotechnol.* **30,** 26–36 (2012).
23. Podust, L. M. & Sherman, D. H. Diversity of P450 enzymes in the biosynthesis of natural products. *Nat. Prod. Rep.* **29,** 1251–1266 (2012).
24. Both, P. *et al.* Whole-cell biocatalysts for stereoselective C–H amination reactions. *Angew. Chem. Int. Ed.* **55,** 1511–1513 (2016).
25. Schrewe, M., Ladkau, N., Bühler, B. & Schmid, A. Direct terminal alkylamino-functionalization via multistep biocatalysis in one recombinant whole-cell catalyst. *Adv. Synth. Catal.* **355,** 1693–1697 (2013).
26. McIntosh, J. A. *et al.* Enantioselective intramolecular C–H amination catalyzed by engineered cytochrome P450 enzymes in vitro and in vivo. *Angew. Chem. Int. Ed.* **52,** 9309–9312 (2013).
27. Hyster, T. K., Farwell, C. C., Buller, A. R., McIntosh, J. A. & Arnold, F. H. Enzyme-controlled nitrogen-atom transfer enables regiodivergent C–H amination. *J. Am. Chem. Soc.* **136,** 15505–15508 (2014).

28. Farwell, C. C., Zhang, R. K., McIntosh, J. A., Hyster, T. K. & Arnold, F. H. Enantioselective enzyme-catalyzed aziridination enabled by active-site evolution of a cytochrome P450. *ACS Cent. Sci.* **1,** 89–93 (2015).
29. Prier, C. K., Hyster, T. K., Farwell, C. C., Huang, A. & Arnold, F. H. Asymmetric enzymatic synthesis of allylic amines: a sigmatropic rearrangement strategy. *Angew. Chem. Int. Ed.* **55,** 4711–4715 (2016).
30. Singh, R., Bordeaux, M. & Fasan, R. P450-catalyzed intramolecular sp^3 C–H amination with arylsulfonyl azide substrates. *ACS Catal.* **4,** 546–552 (2014).
31. Bordeaux, M., Singh, R. & Fasan, R. Intramolecular C(sp^3)–H amination of arylsulfonyl azides with engineered and artificial myoglobin-based catalysts. *Bioorg. Med. Chem.* **22,** 5697–5704 (2014).
32. Svastits, E. W., Dawson, J. H., Breslow, R. & Gellman, S. H. Functionalized nitrogen atom transfer catalyzed by cytochrome P-450. *J. Am. Chem. Soc.* **107,** 6427–6428 (1985).
33. Coelho, P. S. *et al.* A serine-substituted P450 catalyzes highly efficient carbene transfer to olefins *in vivo*. *Nat. Chem. Biol.* **9,** 485–487 (2013).
34. Whitehouse, C. J. C., Bell, S. G. & Wong, L.-L. $P450_{BM3}$ (CYP102A1): connecting the dots. *Chem. Soc. Rev.* **41,** 1218–1260 (2012).
35. Barniol-Xicota, M., Leiva, R., Escolano, C. & Vázquez, S. Synthesis of cinacalcet: an enantiopure active pharmaceutical ingredient (API). *Synthesis* **48,** 783–803 (2016).
36. Bloom, J. D., Labthavikul, S. T., Otey, C. R. & Arnold, F. H. Protein stability promotes evolvability. *Proc. Natl Acad. Sci. USA* **103,** 5869–5874 (2006).
37. Ankner, T. & Hilmersson, G. Instantaneous deprotection of tosylamides and esters with SmI_2/Amine/Water. *Org. Lett.* **11,** 503–506 (2009).
38. Poulos, T. L. Cytochrome P450. *Curr. Opin. Struct. Biol.* **5,** 767–774 (1995).
39. Li, H. & Poulos, T. L. The structure of the cytochrome p450BM-3 haem domain complexed with the fatty acid substrate, palmitoleic acid. *Nat. Struct. Biol.* **4,** 140–146 (1997).
40. Roiban, G.-D. & Reetz, M. T. Expanding the toolbox of organic chemists: directed evolution of P450 monooxygenases as catalysts in regio- and stereoselective oxidative hydroxylation. *Chem. Commun.* **51,** 2208–2224 (2015).
41. Key, H. M., Dydio, P., Clark, D. S. & Hartwig, J. F. Abiological catalysis by artificial haem proteins containing noble metals in place of iron. *Nature* **534,** 534–537 (2016).
42. Srivastava, P., Yang, H., Ellis-Guardiola, K. & Lewis, J. C. Engineering a dirhodium artificial metalloenzyme for selective olefin cyclopropanation. *Nat. Commun.* **6,** 7789 (2015).
43. Hyster, T. K., Knörr, L., Ward, T. R. & Rovis, T. Biotinylated Rh(III) complexes in engineered streptavidin for accelerated asymmetric C–H activation. *Science* **338,** 500–503 (2012).
44. Dydio, P., Key, H. M., Hayashi, H., Clark, D. S. & Hartwig, J. F. Chemoselective, enzymatic C–H bond amination catalyzed by a cytochrome P450 containing an Ir(Me)-PIX cofactor. *J. Am. Chem. Soc.* **139,** 1750–1753 (2017).

Acknowledgements

Our research is supported by the National Science Foundation, Division of Molecular and Cellular Biosciences (grant MCB-1513007) and by funds from the American Recovery and Reinvestment Act (ARRA) through the National Institutes of Health Shared Instrumentation Grant Program (S10RR027203). C.K.P. thanks the Resnick Sustainability Institute for a postdoctoral fellowship. R.K.Z. was supported by a National Science Foundation Graduate Research Fellowship (NSF GRFP; DGE-1144469), is a trainee in the Caltech Biotechnology Leadership Program, and has received financial support from the Donna and Benjamin M. Rosen Bioengineering Center. A.R.B. is funded by a Ruth Kirschstein NIH Postdoctoral Fellowship F32G110851. We thank S. Virgil, J. Kaiser, and R. D. Lewis for experimental assistance, and O. F. Brandenberg, S. C. Hammer, and S. B. J. Kan for helpful discussion and comments on the manuscript.

Author contributions

C.K.P. and R.K.Z. designed, carried out, and analysed all amination experiments, with F.H.A. providing guidance. C.K.P., R.K.Z. and S.B.-C. obtained protein crystals. R.K.Z. and A.R.B. solved the crystal structure. C.K.P. and F.H.A. wrote the manuscript with input from all of the authors.

Additional information

Supplementary information and chemical compound information are available in the online version of the paper. Reprints and permissions information is available online at www.nature.com/reprints. Publisher's note: Springer Nature remains neutral with regard to jurisdictional claims in published maps and institutional affiliations. Correspondence and requests for materials should be addressed to F.H.A.

Competing financial interests

The authors declare no competing financial interests.